DOI: 10.1002/ejic.201000591

Nanothermometers for Transmission Electron Microscopy – Fabrication and Characterization

Chiu-Yen Wang[a] and Lih-Juann Chen*[a]

Keywords: Core–shell nanoparticles / Nanostructures / Nanothermometers / Transmission electron microscopy / Gallium / Gold

The fabrication and characterization of nanothermometers for use in transmission electron microscopy (TEM) are reviewed. Comparisons of different core–shell nanothermometers in terms of the working temperature range, growth conditions, and thermal expansion coefficients are made. The thermal stability of oxide compounds is discussed

Introduction

Temperature is one of the most significant parameters for controlling the fabrication of nanomaterials, as the growth rate and product phase can be varied by changing the temperature.[1–3] Recently, electron microscopes, including scanning electron microscopes and transmission electron microscopes, have been used to elucidate the growth mechanisms of nanomaterials and to prepare nanodevices in situ.[4–18] The length of Si and Ge nanostructures can be precisely controlled down to tens of nanometers by in situ annealing in electron microscopes to yield PtSi/Si/PtSi and Cu_3Ge/Ge/Cu_3Ge nanowires (NWs), which show excellent performance as FET (field-effect transisitor) devices.[10,11] Carbon nanotubes (CNTs) are used as nano test tubes to facilitate Au–Ge interactions on the nanoscale at various temperatures.[18]

Expansion nanothermometers composed of core–shell nanostructures and based on temperature calibration by thermal expansion of metals filled into them are expected to monitor local temperature in electron microscopes.[19–29] In 2002, the Ga-filled carbon nanotube (Ga-CNT) nanothermometer was produced by the chemical vapor deposition (CVD) method, and its effectiveness was demonstrated by Bando and co-workers.[19] Subsequently, the same group also developed several other nanothermometers, including Ga-MgO and In-SiO_x nanotubes, by filling low-melting-point metals (Ga and In) into other nanotubes by a one-step CVD method to overcome the problem of the decomposition of CNTs at temperatures higher than 600–700 °C.[20–23]

For an ideal nanothermometer, there are three crucial aspects, which include stability, accuracy, and reproducibility. These three aspects are important and depend greatly on the properties of the core–shell materials that are used

[a] Department of Materials Science and Engineering, National Tsing Hua University, Hsinchu (30013), Taiwan, Republic of China
Fax: +886-03-5722366
E-mail: ljchen@mx.nthu.edu.tw

Chiu-Yen Wang received B.S. and M.S. degrees in chemistry from Chung Cheng University (2002) and Taiwan University (2004), respectively, and a Ph. D. degree in materials science and engineering from Tsing Hua University Taiwan (2008). She joined Prof. Lih J. Chen's group at Tsing Hua University, Hsinchu, Taiwan, as a postdoctoral fellow in August 2008. Her research interests include the development of nanostructured materials for applications of nanocables as nanothermometers, the study of reactions of Ge nanowires with metal contacts by in situ transmission electron microscopy, as well as the fabrication and characterization of nanodevices with metal-germanide–germanium–metal-germanide heterostructures.

Lih Juann Chen obtained his Ph. D. in physics from the University of California, Berkeley. He is the Distinguished Chair Professor and the President of the National Tsing Hua University. His current research interests are in the synthesis and applications of low-dimensional nanomaterials, atomic scale structures, and dynamic processes of advanced materials, including metallization in integrated circuit devices.

View this journal online at wileyonlinelibrary.com
© 2010 Wiley-VCH Verlag GmbH & Co. KGaA, Weinheim

to make the thermometers. Excluding the resolution limitation of electron microscopes, the precision and accuracy of a nanothermometer are determined by the thermal expansion coefficients (TECs) of both the core and the shell, and the length of the core filling. The reproducibility depends on both the wetting and the chemical reactions of the core and the shell. To measure the temperature in electron microscopes at high temperatures, nanothermometers with chemical and thermal stability are required. As the size is scaled down to the nano range (especially smaller than 10 nm), the physical and chemical properties (including melting point, elasticity, and optical characteristics) of the nanomaterials may be different from those of the bulk materials.[30] *TECs of most low-melting-point metals are between 100 and 150 ppm/°C in the liquid state, and TECs of solid metal oxides are usually less than a few ppm/°C.*[19–29]

Expansion nanothermometers filled with low-melting-point metals have been demonstrated to be useful for in situ TEM. However, the working temperature range of those nanothermometers is still limited by the characteristics of the core and shell materials and the low pressure in the microscope. The sheath should possess a high melting point to resist thermal decomposition and should not react with the core material at high temperatures. On the other hand, it is desired for the core to possess a high boiling point. It is difficult to control uniformity, diameter, and cavity length of nanothermometers prepared by the CVD method. Methods of preparing durable core–shell structures by more facile and controllable approaches for operating in high-vacuum environments in electron microscopes are desirable.

This microreview covers the synthesis of core–shell nanostructures and fabrication of expansion nanothermometers by the CVD method in a furnace at high temperature and by the galvanic displacement reaction at room temperature. In addition, the thermal stability of oxide compounds on the nanoscale and fabrication of core–shell structures with the template procedure are also addressed.

Syntheses of Core–Shell Nanocables

Core–shell nanostructures have been synthesized by many one-step techniques.[31–37] CVD is one of the most common growth method for producing core–shell nanostructures on a large scale. Usually, metal nanoclusters are deposited on a substrate as catalyst to reduce the growth temperature and control the product morphologies through the vapor-liquid-solid (VLS) mechanism. Core–shell nanostructures of Au-silica, Au-Ga_2O_3 and Cr_5Si_3-Si were successfully synthesized by the CVD method in a furnace with Au as catalyst.[32–35]

Two-step template methods, such as CVD without metal catalyst, atomic layer deposition (ALD), template-based electrochemical deposition, and sol–gel processes, have also been used to prepare core–shell nanostructures.[38–48] For example, Ga and O vapors reacted with ZnO NW templates to form ZnO-$ZnGa_2O_4$ core–shell nanostructures by the CVD method, SiO_x-Au and SiO_x-Cu nanocables have been synthesized by using silicon oxide nanowires as templates by metalorganic chemical vapor deposition (MOCVD) and electroless deposition, respectively.[44–46]

Fabrication and Characterization of Expansion Nanothermometers

Liquid-State Nanothermometers

Most core–shell nanocables with low-melting-point cores and chemically stable sheaths were synthesized by the CVD method and demonstrated to be suitable expansion nanothermometers.[19–29] The first core–shell expansion nanothermometer manufactured by CVD, Ga-CNT, was reported by Bando et al. in 2002.[19] This Ga-CNT nanothermometer could read the temperature recorded by the nanothermometer in situ with the help of a scanning electron microscope, even when operated at 10 keV. As changes in the length and diameter of the CNT can be disregarded, the height and TEC of the Ga column in the CNT can be determined by the variation of its volume with temperature. Bando et al. revealed, moreover, that Ga-filled CNT thermometers are fully capable of measuring the temperature in normal air.[23]

After Ga-CNT nanocables, Bando et al. also grew Ga-MgO, In-CNT, and In-silica to tune the range of temperature measurement at ambient temperature and the stability of the nanothermometer at high temperatures. Their previous work displayed that CNTs are prone to fast degradation in air as the temperature reaches approximately 600–700 °C.[20,22,29] The melting point of MgO is 2800 °C, and the liquid range of Ga is wide: from 30 to 2205 °C. Ga-MgO nanocables are expected to be effectively used as nanothermometers in drastic conditions, specially, at very high temperatures.[20] CNT and MgO nanotubes filled with Ga show expansion behavior at nearly room temperature. In addition, indium (m.p. = 156 °C) was also filled into a CNT and a silica nanotube to study its expansion behavior in the liquid state.[21,22,25] As the temperature is lowered, In cannot recover to its initial position in the CNT, and the melting behavior is significantly different from that for a macroscopic state.[21] On the other hand, the VLS-grown In-silica nanotube shows reversible properties, and its range of operation is between 20 and 500 °C.[22]

Alloys should be potentially suitable materials to fill into nanotubes for use as nanothermometers, except for low-melting-point pure metals. Here we use Au(Si)-β Ga_2O_3 nanocables as an example to discuss the growth mechanism and thermal expansion behavior under conditions of in situ TEM.[29]

Fabrication of the Au(Si)-β Ga_2O_3 nanocables was carried out in a horizontal three-zone tube furnace by the CVD method. The mixed powders of Ga_2O_3 and graphite were placed into an alumina crucible positioned at 1100 °C. Silicon (100) coated with 4 nm-thick Au was used as reacting substrate at 700 °C. The growth process took place in an Ar flow during ramping up, and an O_2 flow was intro-

 © 2010 Wiley-VCH Verlag GmbH & Co. KGaA, Weinheim

duced after the set temperature was reached. The growth at set temperature continued for an hour at a fixed pressure of 3.5 Torr.

The composition, morphology, and structure of the product were characterized by SEM, XRD, and TEM. The proposed growth mechanism of the Au(Si)-β Ga_2O_3 core–shell structure is shown in Figure 1. During the growth process, Si will diffuse into Au to form Au(Si) liquid alloy as substrates are heated at a temperature higher than 400 °C. After Ga_2O_3 and Ga vapor are dissolved in the Au(Si) alloy, Ga_2O_3 nanotubes are grown by the VLS mechanism, and Au(Si) columns rise within them as a result of capillary attraction.

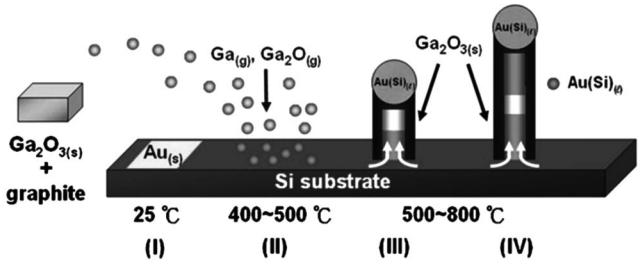

Figure 1. Schematic showing the experimental procedures and physical process of the growth: (I) the Si (001) substrate is coated with 4–8 nm Au film, (II) the heated Au film forms Au–Si alloy nanodots above the Au–Si eutectic point, (III) and (IV) the alloy nanodots serve as a catalyst for the growth of the Ga_2O_3 nanotube. By capillary action, Au(Si) is drawn into the nanotube. Reproduced with permission by the author from ref.[29]

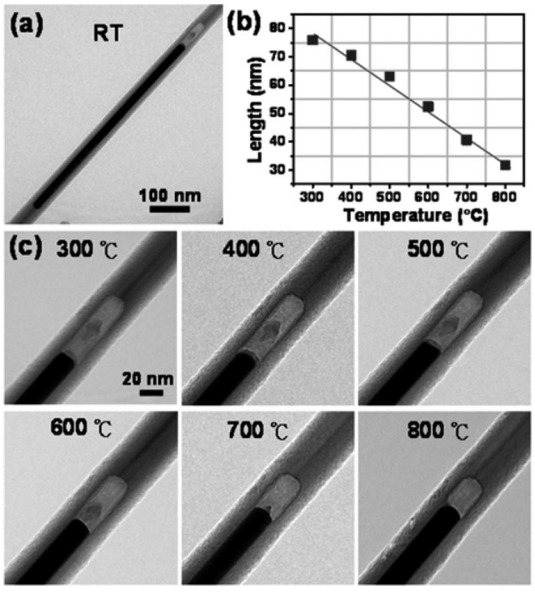

Figure 2. (a) TEM image of a selected Ga_2O_3 nanotube before heating. (b) Distance of the Au filling to the top of the cavity during heating as a function of temperature. (c) TEM images of an Au-filled Ga_2O_3 nanotube while heating at different temperatures. Reproduced with permission by the author from ref.[29]

The thermal expansion behavior of liquid Au(Si) nanowires was studied by in situ TEM. Figure 2 shows the Au(Si)-β Ga_2O_3 nanocable being heated from room temperature to 800 °C. At a temperature higher than 400 °C, the linear expansion of liquid Au(Si) can be observed. Liquefaction of Au(Si) is confirmed by the volume change of the phase transition and the disappearance of the Au diffraction pattern. The TEC (about 150 ppm/°C) of liquid Au(Si) is determined by calculating the length of the NWs at different temperatures. The safe working range of Au(Si)-β Ga_2O_3 nanocable is 300–800 °C.

Solid-State Nanothermometers

Pb-ZnO_x nanocables made by a galvanic displacement reaction are the only available solid-state expansion nanothermometers so far. This is a template-free and spontaneous reaction that proceeds in solution at room temperature. The optimum growth conditions are obtained by using 1 mM lead acetate on Zn foil. The Pb-ZnO nanocables are up to a few hundred micrometers long.[27,28] The filled nanotubes and gaps between the filling materials can be seen from the distinct contrast between the outer shell and the fillings, as shown in Figure 3.

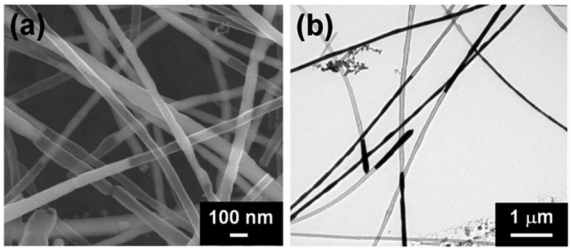

Figure 3. (a) SEM image of Pb-ZnO nanocables showing a distinct contrast for the metal filling inside the nanotubes. (b) TEM image of as-prepared Pb-ZnO nanocables showing segmented Pb fillings inside the ZnO nanotubes. Reproduced from ref.[27]

In situ TEM was used to investigate the thermal expansion properties of solid Pb inside ZnO_x nanocables in real time. Figure 4 demonstrates the thermal expansion behavior in the temperature range 25–300 °C. Figure 4g is a plot of cavity length vs. temperature, with a linear relationship evident for both heating and cooling. The TCE of solid Pb, 30 ± 1.7 ppm/°C, was determined and calculated from the in situ TEM data. The thermal expansion of liquid Pb has also been studied in ZnO_x nanotubes from its melting point to 830 °C.

 © 2010 Wiley-VCH Verlag GmbH & Co. KGaA, Weinheim

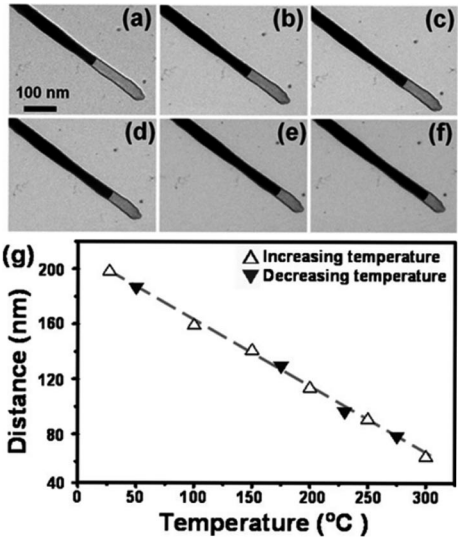

Figure 4. TEM images of a selected Pb-ZnO nanocable, with a Pb filling about 16 μm in length, heated from room temperature to 25 (a), 100 (b), 150 (c), 200 (d), 250 (e), and 300 °C (f), recorded by a video camera in a transmission electron microscope. (g) Plot of cavity length vs. heating temperature. Reproduced from ref.[27]

Discussion and Comparisons of Expansion Nanothermometers

Au(Si)-β Ga_2O_3 core–shell structures made by the CVD method are thermally and chemically stable below the growth temperature. As the working temperature is higher than the growth temperature, the shell usually suffers from thermal decomposition under vacuum. Moreover, the cavity length in the core–shell structure is determined by liquid contraction and phase transition. As a result, it imposes a limitation on the working temperature.

The high-yield and low-cost galvanic displacement reaction has demonstrated the ability to produce Pb-ZnO_x nanocables as solid-state nanothermometers at room temperature. The merit of using a solid-state filling at the required temperature is that it is much less demanding on the integrity of the outer shell. The TEC of bulk solid Pb (δ = 30 ppm/°C) is lower than those of most liquid metals (about 120 ppm/°C). The lengths of solid Pb-ZnO_x nanocables can be up to hundreds of micrometers to enhance the sensitivity of the nanothermometer. Solid Pb-ZnO_x nanocables could be produced at room temperature, and their working temperatures are 30–300 °C. On the other hand, chemical reaction occurred and polycrystalline ZnO_x could not effectively prevent the leakage of liquid Pb at higher temperatures.

Up to the present time, most of expansion nanothermometers have been prepared by the CVD method at high temperatures (above 700–1360 °C) under vacuum. The Au(Si)-β Ga_2O_3 nanocable can be operated up to 800 °C, and the Ga-MgO nanocable has the widest working range (30–694 °C). The TECs of Ga in a CNTs and MgO nanotubes are 95 and 114 ppm/°C, respectively. The variations are caused by the wetting and the difference in TEC among core and shell. Indium (m.p. = 156 °C) has also been filled into CNTs and silica nanotubes to utilize the thermal expansion. The Pb-ZnO_x system is unique, because it is the only nanothermometer operating in the solid state. On the basis of our Au(Si)-β Ga_2O_3 study, a similar concept can be applied to the preparation of Au(Sn)-SnO_2 and Au(In)-In_2O_3 nanocables by the CVD method. Comparisons of different core–shell expansion nanothermometers in terms of the working temperature range, growth conditions, and TEC are listed in Table 1.

Table 1. Comparison of different core–shell structures in terms: melting temperature of the core, growth method, working temperature range, and thermal expansion coefficient (α).[19–23,27–29]

Core–shell nanostructure	Melting temp. of core (°C)	Growth method [Temp.(°C)]	Working temp. range (°C)	α (ppm/°C)
Ga-CNT	29.8	CVD [800]	50–500	95
Ga-MgO	29.8	CVD [850–950]	30–694	114
In-SiO_x	156.7	CVD [750–850]	156–500	–
In-CNT	156.7	CVD [–]	156–400	100–300
Au(Si)-β Ga_2O_3	361	CVD [700]	400–800	150
Pb-ZnO_x	327.4	Galvanic displacement [RT]	RT-300	30

Thermal Stability of Oxide Compounds and Nanothermometer Reinforcement

Expansion nanothermometers are composed of core materials with low melting points and sheaths with high thermal stability. It is important to clarify the thermal decomposition behavior of oxide compounds at high temperature and low pressure. For example, shells of Ga_2O_3 (m.p. = 1780 °C) nanotubes decompose as the temperature is raised to 800 °C, as shown in Figure 2c. As a result, the working temperature of Au(Si)-β Ga_2O_3 expansion nanothermometers is lower than 800 °C.

Melting points of oxide compounds are usually higher than 1000 °C. However, the compounds might decompose below 800 °C under conditions of non-UHV TEM. Figures 5a and c are TEM images of SnO_2 and ZnO NWs (prepared by CVD at 700–800 °C) at room temperature and 750 °C in non-UHV TEM, respectively. The m.p. of SnO_2 is 1630 °C and that of ZnO is 1975 °C, but thermal decomposition occurs at 750 °C and 700 °C (in Figure 5b and d), respectively.

Table 2 lists the melting point, TEC, and thermal stability data of oxide compounds under conditions of non-UHV TEM. Silica nanotubes made by the sol–gel method have also been investigated. For metal oxides, including SiO_x, TiO_x and SnO_x, made by the sol–gel processes, the thickness can be readily controlled.[38,48] Silica possesses an extremely low TEC (0.5–1 ppm/°C) and superior thermal stability in non-UHV TEM.

 © 2010 Wiley-VCH Verlag GmbH & Co. KGaA, Weinheim

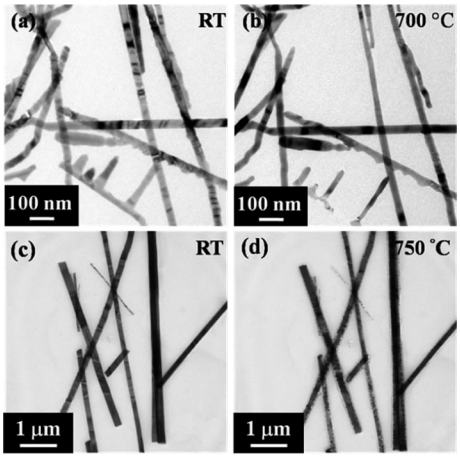

Figure 5. TEM images of ZnO nanowires (a) at room temperature and (b) at 700 °C. TEM images of SnO_2 nanowires (c) at room temperature and (d) after heating to 750 °C.

Table 2. Comparison of melting point, thermal expansion coefficient (α), and thermal stability of oxide compounds under conditions of non-UHV TEM.[27,29,49–53]

	Melting point (°C)	α (ppm/°C)	Limitation (°C)
β-Ga_2O_3	1780	4.6	800
In_2O_3	1910	7–8	700
SnO_2	1630	4.5	750
ZnO	1975	2–4	700
SiO_2	1650	0.5–1	900
WO_3	1473	10–13	800

The advantages of expansion nanothermometers made by the CVD method are the inertness of the core and shell at high temperature. On the other hand, shells are prone to be decomposed. Expansion nanothermometers can be operated at higher temperatures, and the thermal decomposition of the sheath can be restrained if they can be modified with chemically and thermally stable compounds, such as silica. In addition to the sol–gel method, the ALD technique also can be considered to decorate highly chemically resistant and thermally stable compounds (TiO_2, HfO_2, and Al_2O_3) on expansion nanothermometers.[40–43] It is important to minimize chemical reaction between sheath and modified material.

Before core–shell nanocables can be used as expansion nanothermometers for in situ annealing TEM, it is important to develop the process to satisfy the following conditions: (1) filling longer nanowires in the nanotubes to enhance the sensitivity, (2) controlling the ratio of the length of the cavity to the length of the nanowire, and (3) manipulating the nanothermometer to a specific position.

Conclusions

In the past several years, many techniques were developed to fabricate core–shell nanocables. The nanostructures are regarded as the most promising candidates as expansion nanothermometers to monitor the local temperature for in situ electron microscopy. The microreview covers representative examples utilizing in situ transition electron microscopes to demonstrate nanothermometry. Various nanothermometers reported in the literature are compared.

Acknowledgments

The work was supported by the National Science Council through grant no. NSC 98–2221-E-007–104-MY3.

[1] X. S. Fang, C. H. Ye, L. D. Zhang, Y. H. Wang, Y. C. Wu, *Adv. Funct. Mater.* **2005**, *15*, 63–68.
[2] X. S. Fang, C. H. Ye, X. S. Peng, Y. H. Wang, Y. C. Wu, L. D. Zhang, *J. Mater. Chem.* **2003**, *13*, 3040–3043.
[3] Z. W. Pan, Z. R. Dai, L. Xu, S. T. Lee, Z. L. Wang, *J. Phys. Chem. B* **2001**, *105*, 2507–2514.
[4] J. B. Hannon, S. Kodambaka, F. M. Ross, R. M. Tromp, *Nature* **2006**, *440*, 69–71.
[5] S. Kodambaka, J. Tersoff, M. C. Reuter, F. M. Ross, *Science* **2007**, *316*, 729–732.
[6] B. J. Kim, J. Tersoff, S. Kodambaka, M. C. Reuter, E. A. Stach, F. M. Ross, *Science* **2008**, *322*, 1070–1073.
[7] S. Kodambaka, J. Tersoff, M. C. Reuter, F. M. Ross, *Phys. Rev. Lett.* **2006**, *96*, 095105 (1–4).
[8] F. M. Ross, *Mater. Today* **2006**, *9*, 54–55.
[9] S. Kodambaka, J. B. Hannon, R. M. Tromp, F. M. Ross, *Nano Lett.* **2006**, *6*, 1292–1296.
[10] Y.-C. Lin, K.-C. Lu, W.-W. Wu, J.-W. Bai, L. J. Chen, K. N. Tu, Y. Huang, *Nano Lett.* **2008**, *8*, 913–918.
[11] T. Burchhart, A. Lugstein, Y. J. Hyun, G. Hochleitner, E. Bertagnolli, *Nano Lett.* **2009**, *9*, 3739–3742.
[12] K. C. Lu, W. W. Wu, H. W. Wu, C. M. Tanner, J. P. Chang, L. J. Chen, K. N. Tu, *Nano Lett.* **2007**, *7*, 2389–2394.
[13] K. C. Lu, K. N. Tu, W. W. Wu, L. J. Chen, B. Y. Yoo, N. V. Myung, *Appl. Phys. Lett.* **2007**, *90*, 253111 (1–3).
[14] Y. C. Chou, W. W. Wu, S. L. Cheng, B. Y. Yoo, N. Myung, L. J. Chen, K. N. Tu, *Nano Lett.* **2008**, *8*, 2194–2199.
[15] H. C. Hsu, W. W. Wu, H. F. Hsu, L. J. Chen, *Nano Lett.* **2007**, *7*, 885–889.
[16] M. A. van Huis, L. T. Kunneman, K. Overgaag, Q. Xu, G. Pandraud, H. W. Zandbergen, D. Vanmaekelbergh, *Nano Lett.* **2008**, *8*, 3959–3963.
[17] M. A. van Huis, N. P. Young, G. Pandraud, J. F. Creemer, D. Vanmaekelbergh, A. I. Kirkland, H. W. Zandbergen, *Adv. Mater.* **2009**, *21*, 4992–4995.
[18] V. C. Holmberg, M. G. Panthani, B. A. Korgel, *Science* **2009**, *326*, 405–407.
[19] Y. Gao, Y. Bando, *Nature* **2002**, *415*, 599–600.
[20] Y. B. Li, Y. Bando, D. Golberg, Z. W. Liu, *Appl. Phys. Lett.* **2003**, *83*, 999–1001.
[21] Y. Gao, Y. Bando, D. Golberg, *Appl. Phys. Lett.* **2002**, *81*, 4133–4135.
[22] Y. Li, Y. Bando, D. Golberg, *Adv. Mater.* **2004**, *16*, 37–40.
[23] Y. Gao, Y. Bando, Z. W. Liu, D. Golberg, H. Nakanishi, *Appl. Phys. Lett.* **2003**, *83*, 2913–2915.
[24] P. S. Dorozhkin, S. V. Tovstonog, D. Golberg, J. Zhan, Y. Ishikawa, M. Shiozawa, H. Nakanishi, K. Nakata, Y. Bando, *Small* **2005**, *1*,1088–1093.
[25] D. Golberg, Y. B. Li, M. Mitome, Y. Bando, *Chem. Phys. Lett.* **2005**, *409*, 75–80.
[26] J. H. Zhan, Y. Bando, J. Q. Hu, Z. W. Liu, L. Yin, D. Golberg, *Angew. Chem. Int. Ed.* **2005**, *44*, 2140–2144.
[27] C. Y. Wang, N. W. Gong, L. J. Chen, *Adv. Mater.* **2008**, *20*, 4789–4792.
[28] C. Y. Wang, M. Y. Lu, H. C. Chen, L. J. Chen, *J. Phys. Chem. C* **2007**, *111*, 6215–6219.
[29] N. W. Gong, M. Y. Lu, C. Y. Wang, Y. Chen, L. J. Chen, *Appl. Phys. Lett.* **2008**, *92*, 073101 (1–3).

 © 2010 Wiley-VCH Verlag GmbH & Co. KGaA, Weinheim

[30] J. Lee, N. A. Kotov, *Nano Today* **2007**, *2*, 48–51.
[31] Y. Zhang, K. Suenaga, C. Colliex, S. Iijima, *Science* **1998**, *281*, 973–975.
[32] M. S. Hu, H. L. Chen, C. H. Shen, L. S. Hong, B. R. Huang, K. H. Chen, L. C. Chen, *Nat. Mater.* **2006**, *5*, 102–106.
[33] C. H. Hsieh, L. J. Chou, G. R. Lin, Y. Bando, D. Golberg, *Nano Lett.* **2008**, *8*, 3081–3085.
[34] Y. J. Wu, C. H. Hsieh, P. H. Chen, J. Y. Li, L. J. Chou, L. J. Chen, *ACS Nano* **2010**, *4*, 1393–1398.
[35] M. T. Chang, C. Y. Chen, L. J. Chou, L. J. Chen, *ACS Nano* **2009**, *3*, 3776–3780.
[36] D. Moore, J. R. Morber, R. L. Snyder, Z. L. Wang, *J. Phys. Chem. C* **2008**, *112*, 2895–2903.
[37] Y. Jin, D. Y. Yang, D. Y. Kang, X. Y. Jiang, *Langmuir* **2010**, *26*, 1186–1190.
[38] Y. D. Yin, Y. Lu, Y. G. Sun, Y. N. Xia, *Nano Lett.* **2002**, *2*, 427–430.
[39] K. Takahashi, Y. Wang, G. Z. Cao, *J. Phys. Chem. B* **2005**, *109*, 48–51.
[40] Y. Yang, D. S. Kim, M. Knez, R. Scholz, A. Berger, E. Pippel, D. Hesse, U. Gölsele, M. Zacharias, *J. Phys. Chem. C* **2008**, *112*, 4068–4074.
[41] Y. Yang, R. Scholz, A. Berger, D. S. Kim, M. Knez, D. Hesse, U. Gölsele, M. Zacharias, *Small* **2008**, *4*, 2112–2117.
[42] Y. Yang, D. S. Kim, Y. Qin, A. Berger, R. Scholz, H. Kim, M. Knez, U. Gölsele, *J. Am. Chem. Soc.* **2009**, *131*, 13920–13921.
[43] H. J. Fan, U. Gölsele, M. Zacharias, *Small* **2007**, *3*, 1660–1671.
[44] Y. J. Li, M. Y. Lu, C. W. Wang, K. M. Li, L. J. Chen, *Appl. Phys. Lett.* **2006**, *88*, 143102 (1–3).
[45] M. Y. Lu, Y. C. Chang, L. J. Chen, *J. Vac. Sci. Technol. A* **2006**, *24*, 1336–1339.
[46] J. H. Wang, P. Y. Su, M. Y. Lu, L. J. Chen, C. H. Chen, C. J. Chu, *Electrochem. Solid-State Lett.* **2005**, *8*, C9–C11.
[47] C. H. Hsieh, M. T. Chang, Y. J. Chien, L. J. Chou, L. J. Chen, C. D. Chen, *Nano Lett.* **2008**, *8*, 3288–3292.
[48] S. E. Hunyadi, C. J. Murphy, *J. Phys. Chem. B* **2006**, *110*, 7226–7231.
[49] K. D. Kundra, S. Z. Ali, *J. Appl. Crystallogr.* **1970**, *3*, 543–545.
[50] H. Kim, R. C. Y. Auyeung, A. Piqué, *Thin Solid Films* **2008**, *516*, 5052–5056.
[51] I. Blech, U. Cohen, *J. Appl. Phys.* **1982**, *53*, 4202–4207.
[52] H. Tada, A. E. Kumpel, R. E. Lathrop, J. B. Slanina, P. Nieva, P. Zavracky, I. N. Miaoulis, P. Y. Wong, *J. Appl. Phys.* **2000**, *87*, 4189–4193.
[53] C. Rosen, E. Banks, B. Post, *Acta Crystallogr.* **1956**, *9*, 475–476.

Received: May 27, 2010
Published Online: July 15, 2010

 © 2010 Wiley-VCH Verlag GmbH & Co. KGaA, Weinheim